Article

Design and Synthesis of Highly Sensitive Fluorogenic Substrates for Glutathione S-Transferase and Application for Activity Imaging in Living Cells

Yuuta Fujikawa, Yasuteru Urano, Toru Komatsu, Kenjiro Hanaoka, Hirotatsu Kojima, Takuya Terai, Hideshi Inoue, and Tetsuo Nagano

J. Am. Chem. Soc., **2008**, 130 (44), 14533-14543 • DOI: 10.1021/ja802423n • Publication Date (Web): 09 October 2008

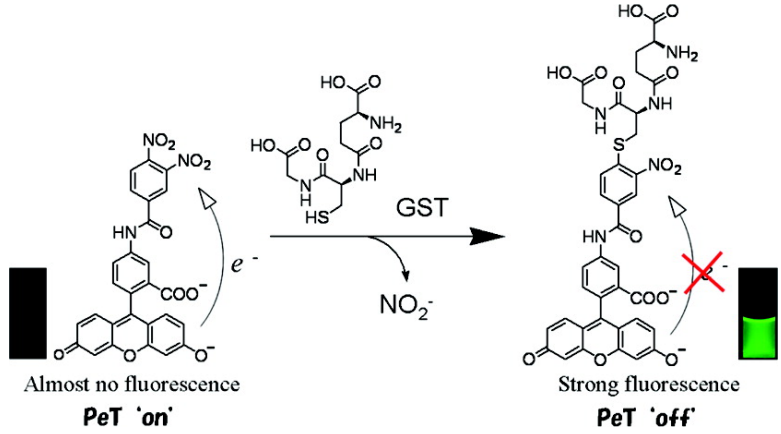

More About This Article

Additional resources and features associated with this article are available within the HTML version:

- Supporting Information
- Access to high resolution figures
- Links to articles and content related to this article
- Copyright permission to reproduce figures and/or text from this article

View the Full Text HTML

J|A|C|S
ARTICLES

Published on Web 10/09/2008

Design and Synthesis of Highly Sensitive Fluorogenic Substrates for Glutathione S-Transferase and Application for Activity Imaging in Living Cells

Yuuta Fujikawa,[†,‡] Yasuteru Urano,[†,§] Toru Komatsu,[†,‡] Kenjiro Hanaoka,[†,‡] Hirotatsu Kojima,[†,‡] Takuya Terai,[†,‡] Hideshi Inoue,[||] and Tetsuo Nagano*[,†,‡]

Graduate School of Pharmaceutical Sciences, The University of Tokyo, 7-3-1 Hongo, Bunkyo-ku, Tokyo 113-0033, Japan, CREST, Japan Science and Technology Agency, Kawaguchi, Saitama, Japan, PRESTO, Japan Science and Technology Agency, Kawaguchi, Saitama, Japan, and School of Life Sciences, Tokyo University of Pharmacy and Life Sciences, 1432-1 Horinouchi, Hachioji, Tokyo 192-0392, Japan

Received April 7, 2008; E-mail: tlong@mol.f.u-tokyo.ac.jp

Abstract: Here we report the development of fluorogenic substrates for glutathione S-transferase (GST), a multigene-family enzyme mainly involved in detoxification of endogenous and exogenous compounds, including drug metabolism. GST is often overexpressed in a variety of malignancies and is involved in the development of resistance to various anticancer drugs. Despite the medical significance of this enzyme, no practical fluorogenic substrates for fluorescence imaging of GST activity or for high-throughput screening of GST inhibitors are yet available. So, we set out to develop new fluorogenic substrates for GST. In preliminary studies, we found that 3,4-dinitrobenzanilide (NNBA) is a specific substrate for GST and established the mechanisms of its glutathionylation and denitration. Using these results as a basis for off/on control of fluorescence, we designed and synthesized new fluorogenic substrates, DNAFs, and a cell membrane-permeable variant, DNAT-Me. These fluorogenic substrates provide a dramatic fluorescence increase upon GST-catalyzed glutathionylation and have excellent kinetic parameters for the present purpose. We were able to detect nuclear localization of GSH/GST activity in HuCCT1 cell lines with the use of DNAT-Me. These results indicate that the newly developed fluorogenic substrates should be useful not only for high-throughput GST-inhibitor screening but also for studies on the mechanisms of drug resistance in cancer cells.

Introduction

Optical detection is one of the most powerful tools to visualize intracellular and extracellular events with high sensitivity and specificity. In the field of chemistry, many fluorescence probes have been developed for metal ions and small organic compounds, as well as for reactive oxygen species (ROS).[1−4] However, there are few nonpeptidic reporter substrates that can directly read out the activity of enzymes, except for hydrolases and kinases. In this paper, we report new fluorogenic substrates that can directly visualize the activity of glutathione S-transferase (GST).

GST is a family of dimeric enzymes involved in phase II detoxification reactions.[5] They participate in a wide range of processes, including xenobiotic biotransformation, drug metabolism, protection against endogenous ROS-induced toxic products, biosynthesis of prostaglandins and steroid hormones, and degradation of aromatic amino acids.[6] Generally, GST catalyzes the conjugation of reduced tripeptide glutathione (GSH) to target molecules, including a wide range of endogenous and exogenous electrophilic substrates. The Pi isoform of GST, named GSTP, was first described as a placental isoform. It seems to play a pivotal role in the carcinogenic process[7−9] and in the development of drug resistance.[10] GSTP is the predominant GST isozyme overexpressed in a wide range of human tumors (gastric, ovarian, nonsmall cell lung, breast, colon, pancreas, lymphoma, etc.).[11] It is usually localized in cytosol, but some reports also describe its localization in the

[†] The University of Tokyo.
[‡] CREST, JST Corporation.
[§] PRESTO, JST Corporation.
[||] Tokyo University of Pharmacy and Life Sciences.

(1) Charier, S.; Ruel, O.; Baudin, J. B.; Alcor, D.; Allemand, J. F.; Meglio, A.; Jullien, L. *Angew. Chem., Int. Ed.* **2004**, *43*, 4785–4788.
(2) Maeda, H.; Katayama, K.; Matsuno, H.; Uno, T. *Angew. Chem., Int. Ed.* **2006**, *45*, 1810–1813.
(3) Miller, E. W.; Chang, C. J. *Curr. Opin. Chem. Biol.* **2007**, *11*, 620–625.
(4) Tang, B.; Xing, Y. L.; Li, P.; Zhang, N.; Yu, F. B.; Yang, G. W. *J. Am. Chem. Soc.* **2007**, *129*, 11666–11667.
(5) Armstrong, R. N. *Chem. Res. Toxicol.* **1997**, *10*, 2–18.
(6) Hayes, J. D.; Flanagan, J. U.; Jowsey, I. R. *Ann. Rev. Pharmacol. Toxicol.* **2005**, *45*, 51–88.
(7) Dang, D. T.; Chen, F.; Kohli, M.; Rago, C.; Cummins, J. M.; Dang, L. H. *Cancer Res.* **2005**, *65*, 9485–9494.
(8) Henderson, C. J.; Smith, A. G.; Ure, J.; Brown, K.; Bacon, E. J.; Wolf, C. R. *Pro. Natl. Acad. Sci. U.S.A.* **1998**, *95*, 5275–5280.
(9) Elsby, R.; Kitteringham, N. R.; Goldring, C. E.; Lovatt, C. A.; Chamberlain, M.; Henderson, C. J.; Wolf, C. R.; Park, B. K. *J. Biol. Chem.* **2003**, *278*, 22243–22249.
(10) Tew, K. D. *Cancer Res.* **1994**, *54*, 4313–4320.
(11) Tew, K. D.; Monks, A.; Barone, L.; Rosser, D.; Akerman, G.; Montali, J. A.; Wheatley, J. B.; Schmidt, D. E. *Mol. Pharmacol.* **1996**, *50*, 149–159.

10.1021/ja802423n CCC: $40.75

nucleus.[12−17] Nuclear GSTP is strongly and inversely correlated to survival of patients with certain types of cancers.[14,18,19] So, in addition to the activity of intracellular GST, its localization is biologically important.

So far, the measurement of GST activity has often been done with the aid of a chromogenic substrate, 2,4-dinitrochlorobenzene (CDNB). But this method suffers from low sensitivity of the chromogenic compound, as well as the fast spontaneous reaction with GSH. Several fluorescent probes or detection methods have been developed for highly sensitive detection of GST activity[20−23] (Figure S1, Supporting Information). But, there is no practical fluorogenic substrate that permits the measurement of GSH/GST activity in living cells. For example, Haugland and colleagues developed PFB-F, which contains a pentafluorobenzoyl moiety (Figure S1a, Supporting Information).[20] The pentafluorobenzoyl moiety of PFB-F is glutathionylated by GST, but the fluorescence properties are not changed by glutathionylation. Thus, the measurement of intracellular total GST activity using CDNB and PFB-F requires careful cell homogenization to avoid degradation by proteases. Not only is there a possibility of misestimating intracellular enzyme activity but also information about the distribution of enzymatic activity is completely lost. Bimanes, such as monobromobimane (mBBr) and monochlorobimane (mBCl)[23,24] are used for detecting intracellular glutathionylation (Figure S1b, Supporting Information). Before reaction, bimanes are fluorescently silent, but once glutathionylated, they become strongly fluorescent. This activation of fluorescence is a useful property for GSH/GST activity imaging, but bimanes are excited in the UV range (<400 nm), which damages cells and tissues of interest, and high background fluorescence is also a problem. Furthermore, as bimanes have high reactivity to GSH in the absence of GST, it is difficult to evaluate GST activity, particularly in living cells. Practical fluorogenic substrates that would make it possible to visualize GSH/GST activity in living cells by means of fluorescence microscopy are still needed, for example, for examining the characteristics of GST-overexpressing cancer cells and cells with the multidrug-resistance phenotype.

Here, we present the first practical fluorogenic substrates for GST, developed on the basis of a rational design strategy. First of all, we explored and found NNBA as a specific substrate for recombinant human GSTP1−1 (hGSTP1). Based on this molecule, we developed new fluorogenic substrates for GST, DNAFs, and DNAT-Me. DNAFs are highly sensitive and useful to evaluate recombinant and lysate GST activity in vitro and DNAT-Me is suitable to visualize the distribution of intracellular GST activity in fluorescence microscopic observation in living cells.

Table 1. Initial Velocity in the Reaction of 10 μM Test Compound with 1.0 mM GSH in the Absence/Presence of hGSTP1

	initial velocity (μM/sec)		
	without hGSTP	with hGSTP	activation[a]
2,4-Chlorodinitrobenzene (CDNB)	0.2	1.6	10.5
Pentafluorobenzanilide (PFBA)[b]	N.D.[c]	N.D.	−
4-Chlor-3-nitrobenzanilide (CNBA)	N.D.	N.D.	−
4-Fluoro-3-nitrobenzanilide (FNBA)	N.D.	0.2	N.C.[d]
3,4-Dinitrobenzanilide (NNBA)	0.02	9.0	528
4-Chloro-3-nitroacetophenone (CNAP)	N.D.	0.2	N.C.
4-Chloro-3-nitrobenzophenone (CNBP)	N.D.	0.2	N.C.

[a] Activation = fold change of initial velocity in with/without GSTP. [b] HPLC confirmed. [c] N.D.; not detectable. [d] N.C.; not calculable.

Results and Discussion

Evaluation of Specific Substrates for GST. Generally, development of enzymatically activated fluorogenic substrates faces two main difficulties. One is to achieve fluorescence activation by specific reaction, and the other is to ensure that the target enzyme recognizes the compound as a specific substrate. In particular, the latter is the first requisite for the development of enzymatically activated fluorogenic substrates. Both nonenzymatic and enzyme-catalyzed nucleophilic conjugations of GSH to CDNB are believed to follow a two-step S_NAr addition/elimination mechanism. Substrates glutathionylated by GST are usually electron-deficient compounds such as CDNB, DCNB (1,2-dichloro-4-nitrobenzene), and other nitro-group-containing aromatic and/or aliphatic compounds. Although these compounds are glutathionylated enzymatically, the noncatalyzed reaction with GSH is relatively fast. So we needed to find a substrate that would specifically undergo GST-catalyzed glutathionylation. For this purpose, we spectrophotometrically examined the reactivity of 7 compounds, including nitrobenzanilide derivatives and nitrobenzene derivatives, toward GSH/hGSTP1 (Figure S2, Supporting Information). The results are summarized in Table. 1. The highest value of activation was seen with NNBA (activation $\approx$ 530). Previously reported compounds, CNAP, CNBP, and a new compound, FNBA, reacted with GSH only in the presence of hGSTP1. This feature is ideal in terms of specific enzyme-catalyzed reaction, but the reaction rates are extremely slow compared with that of NNBA (about 45-fold difference). Threfore, these compounds were not suitable for our purpose. Further, CNBA did not react under these conditions, though it was previously reported to be a substrate for rat GST. Interestingly, the absorbance spectrum of PFBA, which is the reactive moiety of PFB-F, did not change upon reaction with GSH/hGSTP1 under these conditions. Glutathionylation of PFBA was not detectable with HPLC even at 100 μM. As shown in Figure 1A and B, NNBA was recognized by hGSTP1 and had excellent kinetic parameters ($K_M = 23.2\ \mu M$, $k_{cat} = 367\ s^{-1}$, $k_{cat}/K_M = 1.6 \times 10^7\ M^{-1}\ sec^{-1}$) for the hGSTP1-catalyzed reaction (Figure 1C). After completion of the reaction, nitrite was present in quantitative yield in the reaction mixture, suggesting that a nitro group was released

(12) Maguire, N. C.; Drozd, K.; Luff, R. D.; Kantor, R. R. S. *Acta Cytol.* **1991**, *35*, 94–99.
(13) Goto, S.; Ihara, Y.; Urata, Y.; Izumi, S.; Abe, K.; Koji, T.; Kondo, T. *FASEB J.* **2001**, *15*, 2702–2714.
(14) Soh, Y.; Goto, S.; Kitajima, M.; Moriyama, S.; Kotera, K.; Nakayama, T.; Nakajima, H.; Kondo, T.; Ishimaru, T. *Clin. Oncol.* **2005**, *17*, 264–270.
(15) Goto, S.; Kamada, K.; Soh, Y.; Ihara, Y.; Kondo, T. *Jpn. J. Cancer Res.* **2002**, *93*, 1047–1056.
(16) Hall, A. G.; McGuckin, A. G.; Pearson, A. D. J.; Cattan, A. R.; Malcolm, A. J.; Reid, M. M. *J. Clin. Pathol.* **1994**, *47*, 468–469.
(17) Campbell, J. A. H.; Corrigall, A. V.; Guy, A.; Kirsch, R. E. *Cancer* **1991**, *67*, 1608–1613.
(18) Ali-Osman, F.; Brunner, J. M.; Kutluk, T. M.; Hess, K. *Clin. Cancer Res.* **1997**, *3*, 2253–2261.
(19) Allen, T. C.; Granville, L. A.; Cagle, P. T.; Haque, A.; Zander, D. S.; Barrios, R. *Human Pathol.* **2007**, *38*, 220–227.
(20) Arttamangkul, S.; Bhalgat, M. K.; Haugland, R. P.; Diwu, Z. J.; Liu, J. X.; Klaubert, D. H.; Haugland, R. P. *Anal. Biochem.* **1999**, *269*, 410–417.
(21) Svensson, R.; Greno, C.; Johansson, A. S.; Mannervik, B.; Morgenstern, R. *Anal. Biochem.* **2002**, *311*, 171–178.
(22) Zhou, W. H.; Shultz, J. W.; Murphy, N.; Hawkins, E. M.; Bernad, L.; Good, T.; Moothart, L.; Frackman, S.; Klaubert, D. H.; Bulleit, R. F.; Wood, K. V. *Chem. Commun.* **2006**, 4620–4622.
(23) Nauen, R.; Stumpf, N. *Anal. Biochem.* **2002**, *303*, 194–198.
(24) Hulbert, P. B.; Yakubu, S. I. *J. Pharm. Pharmacol.* **1983**, *35*, 384–386.

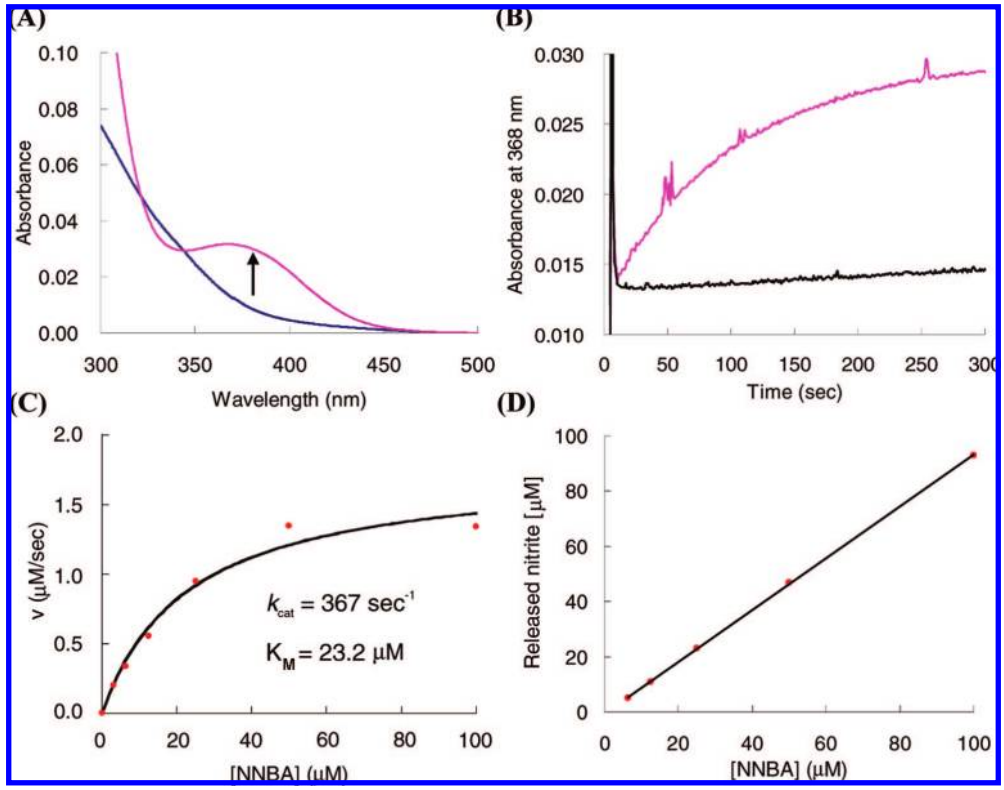

Figure 1. NNBA is good a substrate for GST. (A) Absorbance spectra of 10 μM NNBA and its reaction product in the presence of 1.0 mM GSH and 0.0241 μg/mL hGSTP1 in phosphate-buffered saline (PBS, pH 7.4, 0.2% DMSO as a cosolvent) at 37 °C. The arrow shows the direction of the absorbance changes. (Blue, NNBA; magenta, after reaction for 600 s.) (B) Time courses of reaction of 10 μM NNBA under diffrent conditions (magenta; 1.0 mM GSH and 0.0241 μg/mL hGSTP1, black; 1.0 mM GSH). (C) Michaelis−Menten plot for NNBA. Assay conditions were as follows: 3−100 μM NNBA in PBS (pH 7.4, 1.0% DMSO as a cosolvent) containing 1.0 mM GSH, and 0.241 μg/mL hGSTP1. (D) Linear relation between concentrations of NNBA and released nitrite. After completion of the reaction at various NNBA concentrations (6−100 μM) in (C), nitrite released from NNBA in the reaction mixture was measured using a NO_2/NO_3 Assay Kit-C II (Colorimetric) Griess Reagent Kit (Dojindo, Japan).

as a leaving group with substitution of the sulfhydryl group of GSH (Figure 1D). Which nitro group was eliminated? To address this question, glutathionylated NNBA, named GS-NBA, was synthesized from GSH and NNBA under alkaline conditions. In the ^{1}H NMR spectrum, the chemical shift of the 5-position proton in NNBA was different from in GS-NBA (Figure S3, Supporting Information), suggesting that the 4-nitro group in NNBA is the leaving group. Thus, NNBA is a GST substrate offering a high ratio of enzymatic/nonenzymatic reaction rates, with excellent enzymatic kinetics for the intended purpose. After finding this specific substrate, we next had to consider how the fluorescence can be quenched/activated as a result of the reaction. In general, nitro groups greatly lower the LUMO energy level of aromatic compounds due to their strong electron-withdrawing effect. In a previous report, we showed that an electron-deficient benzene moiety can quench the fluorescence of a fluorophore via an intramolecular photoinduced electron transfer (PeT) process from the excited fluorophore to the electron-deficient benzene moiety (donor-excited PeT; d-PeT).[25−27] In this mechanism, change of the LUMO level on the reaction moiety leads to a change of the fluorescence quantum yield upon specific reaction. Because denitration of

Table 2. Electrochemical Properties of Chromogens for GSTs

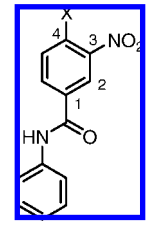

	4-substitutent	E_{red} (V vs SCE)[a]
FNBA	F	−1.08
CNBA	Cl	−1.08
NNBA	NO_2	−0.72
TNBA	SEt	−1.15

[a] Measured in acetonitrile.

NNBA occurs upon glutathionylation, we thought the LUMO level of NNBA would rise. To address this question, we measured the redox potential of NNBA by cyclic voltammetry to estimate the extent of the shift upon reaction with GSH/hGST. As shown in Table 2, NNBA has an exceptionally low reduction potential. Compared with the glutathione-adduct model compound, 4-ethylthio-3-nitrobenzanilide (TNBA) (−1.15 V vs SCE), NNBA has a low reduction potential (−0.72 V vs SCE). This large difference in reduction potential suggests that the fluorescence intensity may be modulated via a d-PeT quenching mechanim upon glutathionylation, when a fluorophore is attached at an appropriate distance from the reactive moiety (Figure 2).

(25) Ueno, T.; Urano, Y.; Setsukinai, K.; Takakusa, H.; Kojima, H.; Kikuchi, K.; Ohkubo, K.; Fukuzumi, S.; Nagano, T. *J. Am. Chem. Soc.* **2004**, *126*, 14079–14085.
(26) Ueno, T.; Urano, Y.; Kojima, H.; Nagano, T. *J. Am. Chem. Soc.* **2006**, *128*, 10640–10641.
(27) Mineno, T.; Ueno, T.; Urano, Y.; Kojima, H.; Nagano, T. *Org. Lett.* **2006**, *8*, 5963–5966.

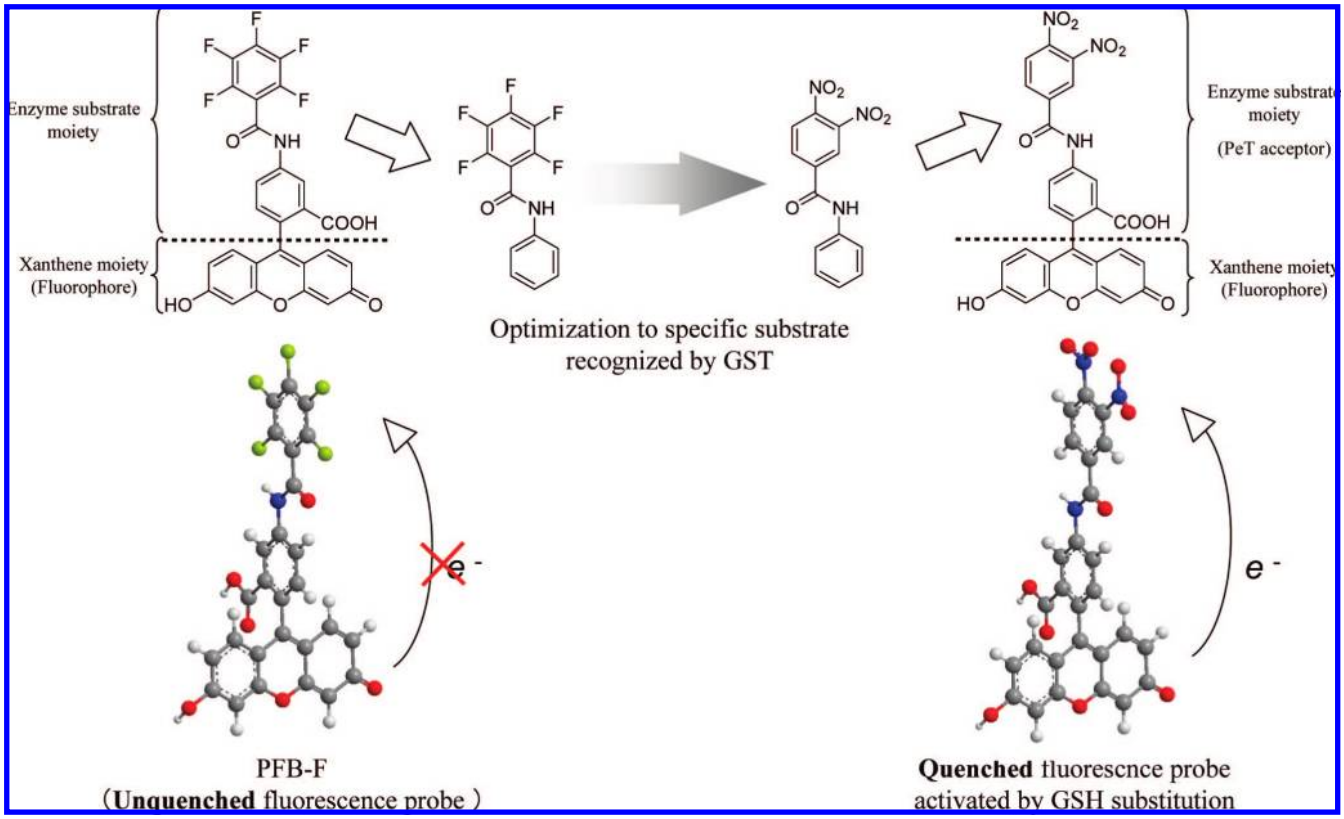

Figure 2. Strategy for the development of GST-catalyzed GSH substitution-activated quenched specific fluorescence probe. The xanthene moiety seems likely to be orthogonal to the enzyme substrate moiety in PFB-F. Therefore, we hypothesized that the xanthene moiety might not interfere with the enzymatic recognition. Thus, pentafluorobenzanilide is expected to be recognized by GST as a substrate. Optimization of this "lead" specific substrate would provide a more reactive and electrochemically specific substrate. The optimized substrate can be recombined with the xanthene moiety to provide a quenched fluorogenic substrate for GST.

Scheme 1. Synthetic Scheme for DNAFs

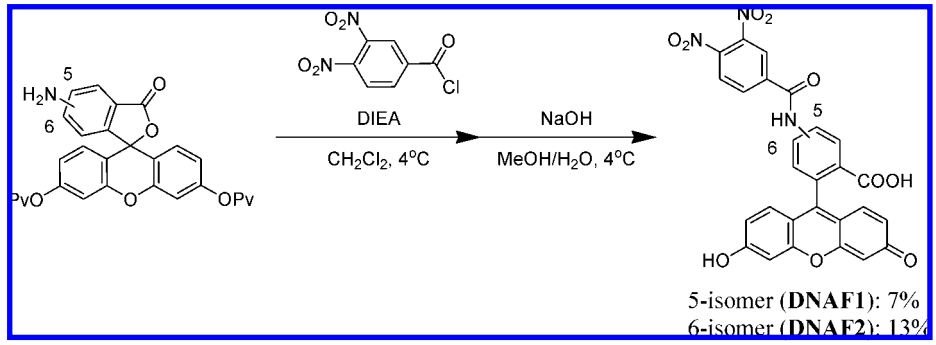

Synthesis of DNAFs. We designed fluorescence probes based on the results of the above reactive moiety search, as illustrated in Figure 1. Synthesis of fluorogenic substrates followed Scheme 1. Because of the availability of aminofluorescein isomers (5 and 6-isomer), we could synthesize dinitrobenzamide fluoresceins, named DNAFs, by means of very simple procedures. Briefly, 3,4-dinitrobenzoic acid was converted to the acid chloride by refluxing in thionyl chloride, followed by reaction with the dipivalic ester-protected aminofluorescein. After deprotection with 2 N NaOH or sodium methoxide in MeOH, the product was purified by means of semipreparative reverse-phase HPLC. We named the 5- and 6-isomer derivatives DNAF1 and DNAF2, respectively.

Photochemical Properties of DNAFs. Photochemical properties of the synthesized compounds are shown in Table 3. As expected, the newly developed DNAFs were good substrates of hGSTP1. That is, a very fast increase of fluorescence intensity was seen upon reaction with GSH/hGSTP1 (Figure 3A). Fluorescence of DNAF1 was highly quenched (the quantum efficacy (Q.E.) was 0.003), but the apparent Q.E. increased to 0.101 after completion of the reaction (Table 3). A 34-fold increase of Q.E. was achieved. The linear correlation of enzyme concentration to initial velocity calculated from the rate of fluorescence increase suggests that the fluorescence increase of DNAF1 is hGSTP1-activity dependent (Figure 3B). HPLC and UPLC−MS analysis revealed that the main fluorescent product is the glutathionylated DNAF1 (Figure 4). Thus, the glutathionylation and subsequent denitration result in strong fluorescence activation (Scheme 2). The specificity of DNAF1 for GSH/hGSTP1 is confirmed in Figure S5 (Supporting Information). The apparent Q.E. values of DNAF2 before and after reaction were 0.008 and 0.257, respectively (Table 3). DNAF2 has a

Table 3. Fluorescence Properties and Kinetic Parameters of mBBr, DNAF1, and DNAF2[a]

substrate	glutathionylation	Abs_{max} (nm)	Em_{max} (nm)	apparent Q.E.	k_2 (GSH) ($M^{-1}sec^{-1}$)	App k_{cat}/K_M ($\times 10^4$ M^{-1} sec^{-1})[b] hGSTA1	hGSTM1	hGSTP1
mBBr	before	394	483	0.009	1.5	258	734	213
	after	388	487	0.191				
DNAF1	before	493	512	0.003	0.2	68	210	1107
	after	492	516	0.101				
DNAF2	before	492	511	0.008	0.09	149	359	1066
	after	492	513	0.257				

[a] Fluorescence quantum yield was calculated using fluorescein (in 0.1 N NaOH aq.) and quinine sulfate (in 0.1 N H_2SO_4) as a standard. Assay was performed in PBS (pH 7.4) at 37 °C. The GSH concentration was 1.0 mM for all substrates. The same protein concentrations as shown in Table 2 were used for DNAFs. In the mBBr assay, protein concentrations were 157 ng/mL, 320 ng/mL, and 24.1 ng/mL for GSTA1, GSTM1, GSTP1, respectively. [b] Apparent k_{cat}/K_M parameter when 1.0 mM GSH used.

somewhat higher Q.E. than DNAF1 and the change of Q.E. upon reaction was about 32-fold. The observation that the absorbance spectra of DNAFs did not change upon reaction suggests that DNAFs are quenched via the PeT mechanism, as expected (Figure S4, Supporting Information). In conclusion, we believe this is the first report of a fluorescence probe utilizing replacement of a nitro group as an off/on mechanism for fluorescence.

Kinetic Parameters of DNAFs. We next evaluated the kinetics of the enzymatic reaction of DNAFs in detail. Table S1 (Supporting Information) summarizes the specific activity of glutathionylation of DNAFs catalyzed by various GST isozymes. Because of quenching at high concentrations of DNAFs (ex. 50 μM), we measured the specific activity at 0.5 μM concentration of DNAFs. DNAF1 appeared to be more susceptible to hGSTP1 compared with DNAF2. The kinetic parameters of mBBr and DNAFs are listed in Table 3. mBBr reacted much faster than DNAFs with GSH in the absence of GST. Thus, DNAFs are superior to known substrates in terms of sensitivity and spontaneous reaction rate with GSH. We anticipate that DNAFs would be well suited for in vitro assays of GST, for example, for high throughput screening (HTS) of GST inhibitors. To test the feasibility of this, we confirmed the inhibitory effect of three known GST inhibitors with DNAF1 as a substrate (Figure S6, Supporting Information). The apparent k_{cat}/K_M values were derived using the Michaelis−Menten relationship at low concentrations (0.5−1.5 μM) of DNAFs: $v/([E]\cdot[S]) = k_{cat}/K_M$, when $K_M > [S]$. All enzymes displayed a linear rate vs substrate concentration behavior in this concentration region. The k_{cat}/K_M values of DNAFs were greater than those of mBBr, particularly in the hGSTP1-catalyzed reaction. Both DNAFs were best with hGSTP1, but the preference for hGSTP1 was greater in the case of DNAF1, the 5-isomer. For DNAF1, k_{cat}/K_M was calculated as 1107×10^4 (sec^{-1} M^{-1}) for hGSTP1, which is slightly lower (about 0.7-fold) than that of NNBA, 1582×10^4 (sec^{-1} M^{-1}). This may be due to the presence of the fluorophore.

Cell Lysate Experiment. Prior to biological application within cells, we tested whether DNAF1 could detect differences of GST activity in cell lysates prepared from seven cell lines: A549 (human lung adenocarcinoma cell line), HuCCT1 (human cholangiocarcinoma cell line), HL-60 (human leukemia cell line), HT1080 (fibrosarcoma cell line), OUS11 (cell line derived from normal tissue of lung cancer patient), HeLa (human cervical adenocarcinoma cell line), and HUVEC (human umbilical vein endothelial cell line). Specific activities of these cell lysates with DNAF1 are listed in Table 4. The highest specific activity in was found in the A549 cell line. Higher GST specific activity in A549 than in the normal counterpart, OUS11, may reflect overexpression of the Pi subtype. Thus, DNAF1 could evaluate GST activities from seven different cell lines. Highly sensitive and specific assay with submicromolar concentrations of DNAF1 and reduced numbers of cells might be suitable to replace the conventional method of GST activity measurement in cell lysates with chromogenic CDNB.

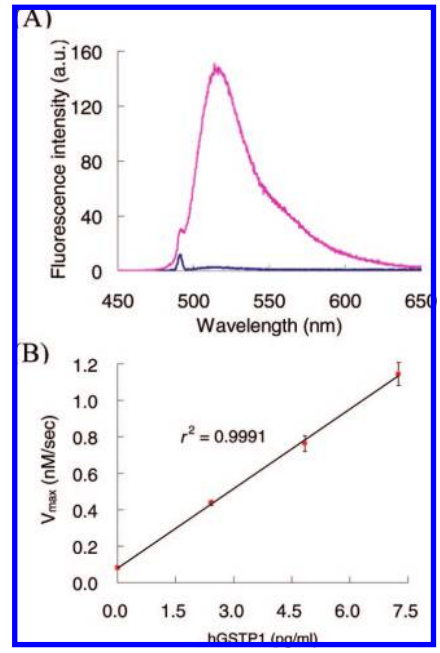

Figure 3. (A) Fluorescence spectra of DNAF1 (0.5 μM in PBS containing 0.1% DMSO as a cosolvent, pH 7.4) before (blue) and after (magenta) addition of 1.0 mM GSH and 0.241 μg/mL hGSTP. (B) Linear relationship of initial velocity of DNAF1 fluorescence increase to concentration of hGSTP1.

Design, Synthesis, and Evaluation of Membrane-Permeable Derivative of DNAF1. DNAF1 is plasma membrane-impermeable due to the moderate hydrophilicity of the fluorescein moiety. So, for application to living cells, we require a method for introduction of DNAF1 into the cells. One approach is to use a protecting group that is cleaved within the cell. In general, hydrophilic fluorescence probes are introduced into cells using protecting groups, such as acetoxymethyl group for carboxylic acid,[28] or acetate ester for phenol, which are hydrolyzed by intracellular esterases. But we felt that this approach is not suitable in the present case because of the possible complex effect of the ester hydrolysis process on the fluorescence increase arising from the reaction with GSH/GST. Another approach is to use the more hydrophobic TokyoGreen (TG) scaffold, which might be better suited for the imaging of GST/GSH activity in living cells. So, we designed and synthesized the TokyoGreen derivative of DNAF1. According to the general synthetic procedure of TGs, we attempted halogen-lithium exchange reaction with the iodonitrobenzene derivative, but this was unsuccessful. We thought the failure of the synthesis might have been due to the presence of the nitro group, and tried the procedure reported by Peterson and co-workers.[29] DNAT-Me was synthesized in 6 steps (Scheme 3). Following reduction to obtain 2-methyl-4-nitrobenzyl alcohol (**1**) from the corresponding benzoic acid as a starting material, oxidation by PCC gave

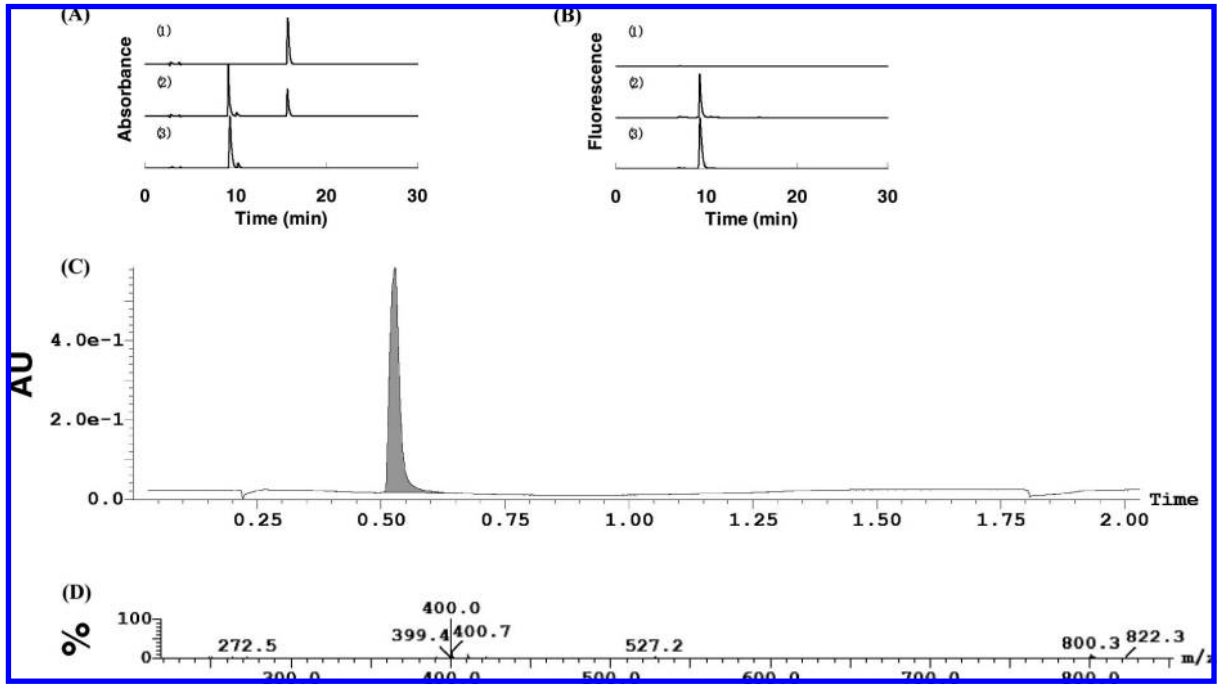

Figure 4. Confirmation of product formation by means of HPLC and LC-MS. HPLC chromatograms with absorbance (A) and fluorescence detection (B). ((1) Before reaction, (2) at 50 s after addition of hGSTP, (3) at 600 s (after completion of the reaction)). Reaction was performed with hGSTP (0.0723 μg/mL), reduced GSH (1.0 mM), and DNAF (100 μM) in PBS (pH 7.4) (1.0% DMSO as a cosolvent) at 37 °C. Absorbance was detected at 490 nm, and fluorescence was detected at 514 nm with excitation at 490 nm. The HPLC conditions: linear gradient (eluent, 0 min 16% CH_3CN/0.1 M TEAA aq. $\approx$ 20 min, 80% CH_3CN/0.1 M TEAA aq.; flow rate = 1.0 mL/min). (C) UPLC−MS chromatogram with absorbance detection at 490 nm of sample (3) in HPLC analysis. (D) Mass spectrum of the peak at 5.3 min and corresponding *m/z* values analyzed by mass spectrometry in the negative ion mode. UPLC conditions: eluent, 0 min 5% CH_3CN/5 mM TEAA aq. $\approx$ 1.00 min, 95% CH_3CN/5 mM TEAA aq. $\approx$ 1.50 min, 5% CH_3CN/5 mM TEAA aq. $\approx$ 1.51 min, 5% CH_3CN/5 mM TEAA aq. MS Scan: scan time 0.10 s, cone voltage; 30.0 V.

Scheme 2. GST-Catalyzed Glutathionylation of DNAF1

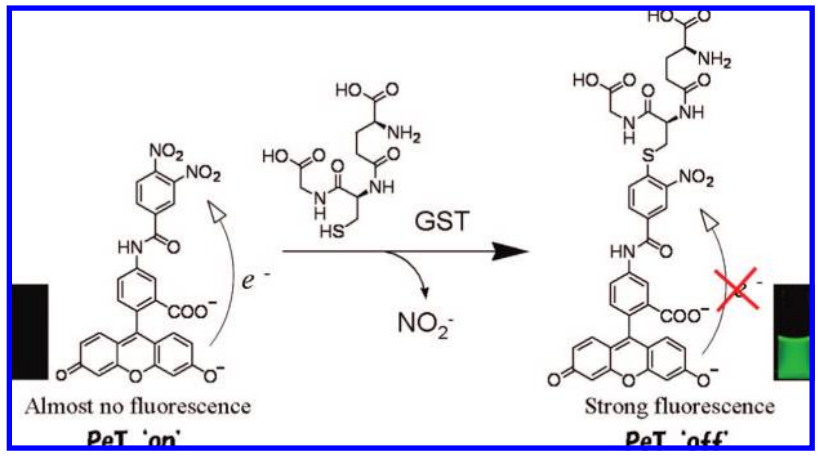

Table 4. Specific Activity of GST[a]

cell line	A549	HuCCT1	HL60	HT1080	OUS11	HUVEC	HeLa
GST activity (pmol/sec/mg protein)	37.5 ±5.34	23.5 ±2.2	10.0 ±0.4	9.5 ±1.8	6.2 ±1.2	3.8 ±0.3	1.7 ±0.6

[a] GST activity was measured using DNAF1 in total cell lysates as described in Materials and Methods. The enzymatic activity was normalized for protein concentration and is shown as specific activity (pmol/sec/mg protein). Data are means of three independent analysis.

2-methyl-4-nitrobenzaldehyde (**2**) in relatively high yield. Condensation with resorcinol was employed the reported conditions, except for the use of excess resorcinol. Polymerization occurred at the ratio of aldehyde **2**: resorcinol = 1:2. The difference between our result and that of Peterson may be due to the absence/presence of a 4-substituent in resorcinol. Therefore, we used an excess of resorcinol to avoid side reaction. This condensation afforded triarylmethane **3** in 40% yield. Then, **3** was refluxed with excess TsOH to afford crude 2-Me-4-NO_2-TG (**4**), which was reduced to 2-Me-4-NH_2-TG (**5**) in 3% yield from **3** (two steps). The desired product was thus synthesized by almost the same procedure as DNAFs in 8% yield, and was designated DNAT-Me. The fluorescence increase of DNAT-Me in PBS (pH 7.4) containing 1.0 mM GSH and hGSTM1 at 37 °C is shown in Figure 5. The Q.E. of DNAT-Me is 0.009, somewhat higher than that of DNAF1, and increased to 0.204 after completion of the reaction in the presence of GSH and hGSTP1. Although the activation ratio of about 23 is less than that of DNAF1 (about 34-fold), we think it is sufficient

Scheme 3. Synthetic Scheme of DNAT-Me

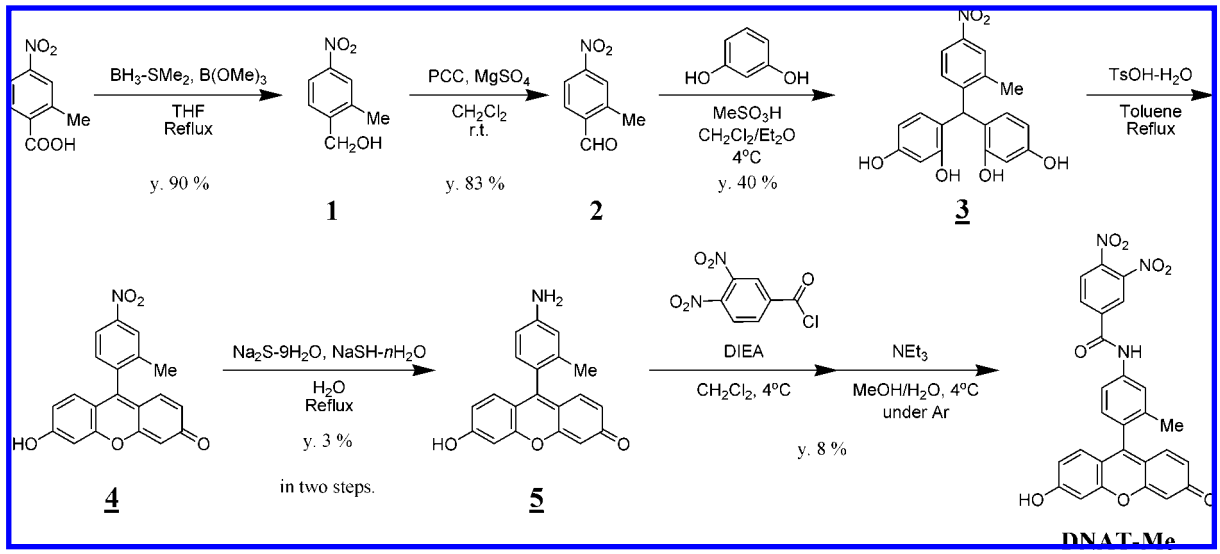

to detect intracellular GSH/GST activity. Next, we evaluated the membrane permeability of DNAT-Me with DNAF1 using HL60 cells. DNAT-Me had a very low Q.E. before glutathionylation, but its entry into cells could be confirmed by highly sensitive flow cytometric analysis. As shown Figure 5B, even after 30 s, higher fluorescence intensity was observed in HL60 cells incubated with DNAT-Me was seen with DNAF1, which showed almost the same intensity as nontreated cells. This suggests that DNAT-Me has high membrane permeability, and that extra-/intracellular equilibrium is rapidly attained. A high intracellular concentration of DNAT-Me should increase the probability of collision with GSTs in the cytoplasm, leading to rapid formation of the fluorescent GS-adduct.

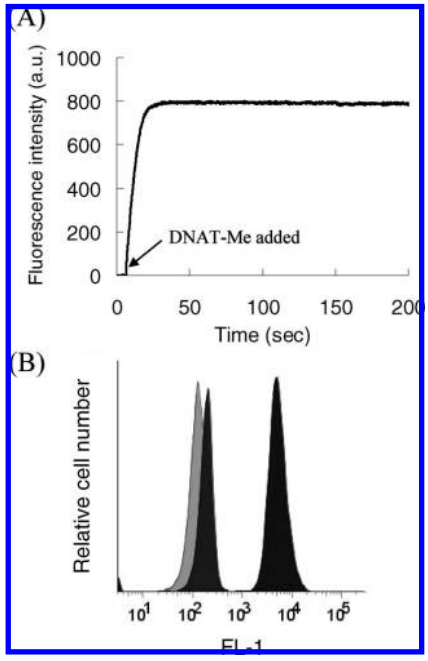

Figure 5. Membrane-permeable fluorogenic substrate, DNAT-Me. (A) Fluorescence increase of DNAT-Me in PBS (pH 7.4, 0.1% DMSO as a cosolvent), containing 1.0 mM GSH, and hGSTM1 (1.569 μg/mL) at 37 °C. Excitation and emission wavelengths were 490 and 514 nm, respectively. (B) High permeability of DNAT-Me. HL60 cells (5.0×10^5 cells/mL) were mixed with 0.5 μM DNAF1 or DNAT-Me in PBS after 30 s and evaluated with a BD LSR II flow cytometer. The gray peak represents untreated samples. Blue and green represent 0.5 μM of DNAT-Me and DNAF1, respectively.

Visualization of GSH/GST Activity in Living Cells by Fluorescence Microscopy. In the lysate experiment, we found that the activity of the GSH/GST system is high in cholangiocarcinoma cell line HuCCT1. Cholangiocarcinoma is a cancer that is highly resistant to various anticancer drugs, and has a poor prognosis.[30−32] Nakajima and colleagues reported that GSTP1−1 is a resistance factor for anticancer drugs in cholangiocarcinoma.[33] In particular, high nuclear GSTP activity is a poor prognostic factor. So we investigated whether nuclear localization of GST activity in HuCCT1 could be imaged by fluorescence microscopy. Cultured cells were washed once with PBS and incubated with 2 μM DNAT-Me for 15 min. As shown in Figure 6, a strong fluorescence signal was seen in the nucleus. HPLC analysis confirmed that the fluorescent product of DNAT-Me was the same GS-adduct as the reaction with GSH/hGSTP1 (Figure S7, Supporting Information). The nuclear localization of high fluorescence was also confirmed by confocal microscopic observation after coincubation with a nuclear-specific dye, SYTO-red (Figure 7). GSH-depleting agent, *N*-ethylmaleimide (NEM), abolished the fluorescence, which confirmed that the nuclear fluorescence signal can be attributed to the GS-adduct (Figure S8, Supporting Information). It has been reported that nuclear localization of GSTP in uterine cancer[34] and glioma cells[18] is negatively correlated with patients' survival. Goto and colleagues demonstrated that this negative correlation was at least partly due to the effect of nuclear GSTP in protecting DNA against damage by anticancer drugs and lipid peroxides.[13,35] Because cholangiocarcinoma is a highly resistant to various

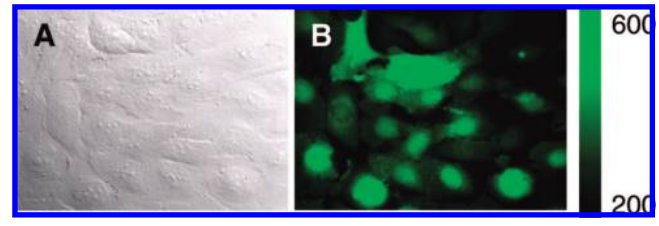

Figure 6. Fluorescence microscopic images of living HuCCT1 cells. (A) Brightfield and (B) fluorescence image of cells incubated with 2 μM DNAT-Me for 15 min at 37 °C. Exposure time was 300 ms, and ND was 25%.

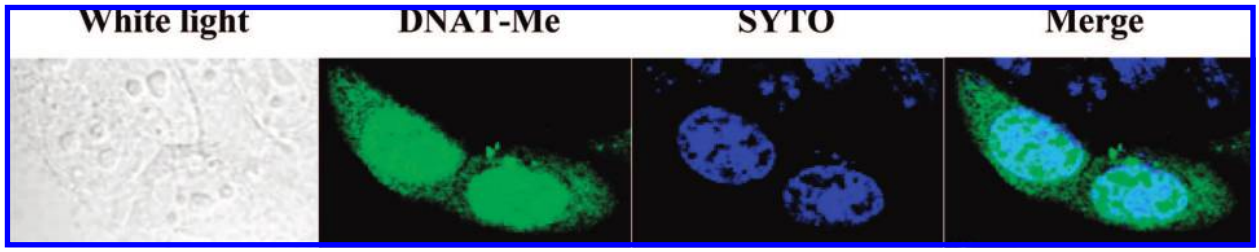

Figure 7. Confocal microscopic imaging of DNAT-Me and SYTO-loaded HuCCT1 cells. HuCCT1 cells were pretreated with 5 μM CCCP in HBSS for 15 min at 37 °C. Then, the medium was changed to fresh HBSS containing DNAT-Me (2 μM), SYTO (1 μM), and CCCP (5 μM), and incubation was continued 15 min. The cells were washed with PBS twice and fluorescence images were aquired through FITC and Cy5 filters for DNAT-Me and SYTO, respectively.

anticancer drugs, the visualization of the nuclear GSTP activity in HuCCT1 with DNAT-Me is of considerable interest and confirms the utility of this membrane-permeable fluorogenic substrate. This is first report of fluorescence imaging of the intracellular distribution of GST activity using an activatable fluorogenic substrate.

Conclusion

We have developed the first off/on-type fluorogenic substrates for GSTs, DNAFs and DNAT-Me, and applied the latter for imaging GST activity in living cells. GST is of clinical interest, because it is overexpressed in various type of cancer cells and is involved in drug resistance. Nevertheless, no practical fluorescence probe for GST activity has been available. We designed and synthesized fluorogenic substrates with an off/on fluorescence switching mechanism based on the replacement of a nitro group with GSH. The DNAFs, have excellent kinetic parameters for multiwell plate experiments. GSTP is an important inhibitor of JNK activity and may function as a regulator of cell proliferation and apoptosis.[9,36,37] The ability of GSTP1 to inhibit JNK appears to be dependent upon the presence of GSTP1 monomer in the cytosol of cells.[38] So GSTP inhibitors are candidate anticancer agents,[39] and indeed many GSTP-selective inhibitors have been developed.[40−42] However, the lack of a high-through put assay format has restricted the development of GST subtype-selective inhibitors. DNAFs are markedly superior to known substrates (such as CDNB and mBBr), especially in terms of sensitivity, and should be suitable for high-throughput screening. The membrane-permeable variant DNAT-Me is available for imaging GST activity in living cells, and was used to visualize high GST activity, possibly due to the Pi subtype, in the nucleus of HuCCT1 cells under a fluorescence microscope. Fluorescence imaging of GSH/GST activity is expected to be useful in many fields, such as obtaining biological insights into drug-resistance phenotypes with high spatio-temporal resolution, and in diagnosis for the detection of GST-overexpressing preneoplastic foci and drug resistance. Further studies on the biological applications of DNAFs and DNAT-Me are in progress.

Experimental Section

Materials and General Instrumentation. General chemicals were purchased from Tokyo Chemical Industries, Wako Pure Chemical, or Aldrich Chemical Co., and were used without further purification. Special chemicals were DMSO (fluorometric grade, Dojindo) and TBAP (electrochemical grade, Fluka). All solvents were used after appropriate distillation or purification. NMR spectra were recorded on a JNM-LA300 (JEOL) instrument at 300 MHz for ^{1}H NMR and 75 MHz for ^{13}C NMR and on a JNM-LA400 (JEOL) instrument at 400 MHz for ^{1}H NMR and 100 MHz for ^{13}C. ESI mass spectra were measured with a JMS-T100LC AccuToF (JEOL). UV−visible spectra were obtained on a Shimadzu UV-1600. Fluorescence photometric studies were performed on a Hitachi F4500.

Cyclic Voltammetry. Cyclic voltammetry was performed as reported.[26]

HPLC Analysis. HPLC analysis was performed on an Inertsil ODS-3 (4.6 × 250 mm) column using an HPLC system composed of a pump (G1312A, Agilent) and a detector (G1315B or G1321A, Agilent). In the LC−MS experiment to analyze the reaction mixture of DNAF1 and GSH in the presence of recombinant human GSTP1−1, LC analysis was done with an Inertsil ODS-3 (2.1 × 150 mm) column using a system composed of a pump (G1312A, Agilent) and a detector (G1314A, Agilent).

Synthesis of Compounds. 4-Fluoro-3-nitrobenzanilide (FNBA). To a solution of oxalyl chloride (745 mg, 5.87 mmol) in 15 mL of CH_2Cl_2, DMF (457 μL, 5.87 mmol) was added. This solution was stirred for 10 min at −20 °C, then 4-fluoro-3-nitrobenzoic acid (249 mg, 1.35 mmol) was added. Stirring was continued for 30 min, then 10 mL of a CH_2Cl_2 solution of aniline (124 μL, 1.35 mmol) and DIEA (1.2 mL, 7.22 mmol) was added at −20 °C. The mixture was stirred for 2.5 h at room temperature, then, after confirmation of disappearance of the starting materials, evaporated to dryness. The residue was poured into AcOEt (100 mL). The organic solution was washed with H_2O (100 mL × 3) and brine, dried over anhydrous Na_2SO_4, and filtered. The filtrate was evaporated to dryness. The residue was purified by a preparative TLC (AcOEt/

(28) Tsien, R. Y. *Nature* **1981**, *290*, 527–528.
(29) Mottram, L. F.; Maddox, E.; Schwab, M.; Beaufils, F.; Peterson, B. R. *Org. Lett.* **2007**, *9*, 3741–3744.
(30) Patel, T. *Hepatology* **2001**, *33*, 1353–1357.
(31) Isa, T.; Kusano, T.; Shimoji, H.; Takeshima, Y.; Muto, Y.; Furukawa, M. *Am. J. Surg.* **2001**, *181*, 507–511.
(32) Okuda, K.; Nakanuma, Y.; Miyazaki, M. *J. Gastroenterol. Hepatol.* **2002**, *17*, 1049–1055.
(33) Nakajima, T.; Takayama, T.; Miyanishi, K.; Nobuoka, A.; Hayashi, T.; Abe, T.; Kato, J.; Sakon, K.; Naniwa, Y.; Tanabe, H.; Niitsu, Y. *J. Pharmacol. Exp. Ther.* **2003**, *306*, 861–869.
(34) Shiratori, Y.; Soma, Y.; Maruyama, H.; Sato, S.; Takano, A.; Sato, K. *Cancer Res.* **1987**, *47*, 6806–6809.
(35) Kamada, K.; Goto, S.; Okunaga, T.; Ihara, Y.; Tsuji, K.; Kawai, Y.; Uchida, K.; Osawa, T.; Matsuo, T.; Nagata, I.; Kondo, T. *Free Radical Biol. Med.* **2004**, *37*, 1875–1884.
(36) Bernardini, S.; Bernassola, F.; Cortese, C.; Ballerini, S.; Melino, G.; Motti, C.; Bellincampi, L.; Iori, R.; Federici, G. *J. Cell. Biochem.* **2000**, *77*, 645–653.
(37) Gilot, D.; Loyer, P.; Corlu, A.; Glaise, D.; Lagadic-Gossmann, D.; Atfi, A.; Morel, F.; Ichijo, H.; Guguen-Guillouzo, C. *J. Biol. Chem.* **2002**, *277*, 49220–49229.
(38) Adler, V.; Yin, Z. M.; Fuchs, S. Y.; Benezra, M.; Rosario, L.; Tew, K. D.; Pincus, M. R.; Sardana, M.; Henderson, C. J.; Wolf, C. R.; Davis, R. J.; Ronai, Z. *EMBO J.* **1999**, *18*, 1321–1334.
(39) Tew, K. D. *Biochem. Pharmacol.* **2007**, *73*, 1257–1269.
(40) Lyttle, M. H.; Hocker, M. D.; Hui, H. C.; Caldwell, C. G.; Aaron, D. T.; Engqvistgoldstein, A.; Flatgaard, J. E.; Bauer, K. E. *J. Med. Chem.* **1994**, *37*, 189–194.
(41) Burg, D.; Mulder, G. J. *Drug Metab. Rev.* **2002**, *34*, 821–863.
(42) Ang, W. H.; De Luca, A.; Chapuis-Bernasconi, C.; Juillerat-Jeanneret, L.; Lo Bello, M.; Dyson, P. J. *ChemMedchem* **2007**, *2*, 1799–1806.

n-hexane = 1/1) to afford the title compound 29.6 mg (8% yield, slight yellowish powder). ^{1}H NMR (300 MHz, DMSO-d_6) δ: 10.57 (1H, s), 8.73 (1H, dd, J = 7.2, 2.3 Hz), 8.38 (1H, ddd, J = 8.7, 4.2, 2.20 Hz), 7.73−7.80 (3H, m), 7.37 (2H, t, J = 8.0 Hz), 7.13 (1H, t, J = 7.4 Hz) ^{13}C NMR (75 MHz, DMSO-d_6) δ: 162.1, 138.3, 136.4, 135.4, 131.4, 128.4, 125.5, 123.9, 120.3, 118.5, 118.3 HRMS (ESI−TOF) m/z Found 259.0506 [M − H]$^-$, calculated 259.0519 (−1.26 mmu).

4-Chloro-3-nitrobenzanilide (CNBA). To a solution of 4-chloro-3-nitrobenzoyl chloride (327 mg, 1.49 mmol) in 8 mL of dioxane, aniline (272 μL, 2.98 mmol) was added dropwise with stirring at room temperature. After 10 min, a white residue appeared, and the mixture was poured into AcOEt (100 mL). The organic solution was washed with H_2O (50 mL × 3) and brine, dried over anhydrous Na_2SO_4, and filtered. The filtrate was evaporated to dryness. The residue was purified on a silica gel column (AcOEt/n-hexane = 5/1) to afford the title compound, 377 mg (91% yield, slight yellowish solid). ^{1}H NMR (300 MHz, DMSO-d_6) δ: 10.53 (1H, s, br), 8.62 (1H, d, J = 2.2 Hz), 8.25 (1H, dd, J = 8.4, 2.2 Hz), 7.96 (1H, d, J = 8.4 Hz), 7.75 (2H, m), 7.37 (2H, m), 7.13 (2H, m) ^{13}C NMR (75 MHz, DMSO-d_6) δ: 162.4, 147.3, 138.5, 134.9, 132.8, 131.9, 128.7, 128.0, 124.9, 124.9, 124.2, 120.5 HRMS (ESI−TOF) m/z Found 464.2350 [M − H]$^-$, calculated 275.0220 for $C_{13}H_8ClN_2O_3$ (−0.38 mmu). Anal. Calcd for $C_{13}H_9ClN_2O_3$: N, 10.13; C, 56.43; H, 3.28, found N, 10.14; C, 56.53; H, 3.42.

4-Ethylthio-3-nitrobenzanilide (TNBA). To a solution of sodium ethanethiolate (54.7 mg, 0.65 mmol) in 5 mL of HMPA, CNBA (183.6 mg, 0.66 mmol) in 5 mL of HMPA was added dropwise. The mixture was stirred overnight at room temperature, then poured into AcOEt (100 mL). The organic solution was washed with H_2O (100 mL × 3) and brine, dried over anhydrous Na_2SO_4, and filtered. The filtrate was evaporated to dryness. The residue was purified by a preparative TLC (AcOEt/n-hexane = 1/1) to afford the title compound 52.3 mg (26% yield, yellow powder). ^{1}H NMR (300 MHz, DMSO-d_6) δ: 10.51 (1H, s), 8.80 (1H, d, J = 2.0 Hz), 8.26 (1H, dd, J = 8.5, 1.9 Hz), 7.75−7.79 (3H, m), 7.37 (2H, t, J = 7.98 Hz), 7.12 (1H, t, J = 7.4 Hz), 3.15 (2H, q, J = 7.3 Hz), 1.31 (3H, t, J = 7.3 Hz) ^{13}C NMR (75 MHz, DMSO-d_6) δ: 162.9, 145.0, 140.8, 138.7, 132.7, 131.0, 128.7, 127.2, 125.1, 124.0, 120.5, 25.5, 12.8 HRMS (ESI−TOF) m/z Found 301.0660 [M − H]$^-$, calculated 301.0647 for $C_{15}H_{13}N_2O_3S$ (+1.27 mmu).

3,4-Dinitrobenzanilide (NNBA). To a solution of oxalyl chloride (1.17 g, 9.2 mmol) in 15 mL of CH_2Cl_2, DMF (717 μL, 9.2 mmol) was added. The mixture was stirred for 10 min at −20 °C, then a CH_2Cl_2/THF (1:1) solution (20 mL) of 3,4-dinitrobenzoic acid (777 mg, 3.7 mmol) was added. Stirring was continued for 30 min, then a solution of aniline (334 μL, 3.7 mmol) and DIEA (1.2 mL, 7.3 mmol) in 10 mL of THF was added at −20 °C. The mixture was stirred for 1 h at room temperature, then after confirmation of disappearance of the starting materials, evaporated to dryness. The residue was poured into CH_2Cl_2 (100 mL). The organic solution was washed with H_2O (100 mL x 3) and brine, dried over anhydrous Na_2SO_4, and filtered. The filtrate was evaporated to dryness. The residue was purified on a silica gel column (CH_2Cl_2) to afford the title compound, 299.6 mg (29% yield, slight yellowish powder). ^{1}H NMR (300 MHz, DMSO-d_6) δ: 10.78 (1H, s, br), 8.80 (1H, d, J = 1.7 Hz), 8.55 (1H, dd, J = 8.3, 1.7 Hz), 8.47 (1H, d, J = 8.3 Hz), 7.81 (2H, d, J = 8.2 Hz), 7.39−7.49 (2H, m), 7.19−7.24 (1H, m) ^{13}C NMR (75 MHz, DMSO-d_6) δ: 161.8, 143.3, 141.6, 139.8, 138.3, 133.8, 128.8, 126.0, 124.9, 124.5, 120.5 HRMS (ESI−TOF) m/z Found 286.0462 [M − H]$^-$, calculated 286.0464 for $C_{13}H_8N_3O_5$ (−0.18 mmu).

DNAF1. 3,4-Dinitrobenzoic acid (148 mg, 0.70 mmol) was suspended in 10 mL of thionyl chloride, and a catalytic amount (a few drops, via a Pasteur pipet) of DMF was added. The mixture was refluxed for 2.5 h. An excess of toluene was added to the reaction mixture, which was then evaporated in vacuo to dryness. The residue was dissolved in 10 mL of CH_2Cl_2, and cooled to −5 °C. A CH_2Cl_2 (5 mL) solution of 5-aminofluorescein dipivaloyl (336 mg, 0.652 mmol) and DIEA (260 μL, 1.56 mmol) was added dropwise, and the reaction mixture was stirred for 4 h at room temperature. The solvent was removed and the residue was redissolved in 10 mL of MeOH, then 10 mL of aqueous 2 N NaOH was added dropwise with stirring overnight at ambient temperature. The reaction was quenched by the addition of 8 mL of aqueous 2 N HCl. The residue was purified by means of preparative reverse-phase HPLC to give the title compound, 27 mg (7.2% yield, orange solid). ^{1}H NMR (300 MHz, DMSO-d_6) δ: 11.10 (1H, s), 10.11 (1H, br), 8.78 (1H, d, J = 1.7 Hz), 8.53 (1H, dd, J = 8.4, 1.7 Hz), 8.43−8.47 (m, 2H), 8.07 (1H, dd, J = 8.4, 1.8 Hz), 7.31 (1H, d, J = 8.4 Hz), 6.67 (2H, d, J = 2.2 Hz), 6.62 (2H, d, J = 8.6 Hz), 6.55 (2H, dd, J = 8.7, 2.3 Hz) ^{13}C NMR (100 MHz, DMSO-d_6) δ: 168.5, 162.4, 159.5, 151.9, 148.0, 143.5, 141.7, 140.0, 139.4, 134.0, 129.1, 127.6, 126.9, 126.2, 125.1, 124.7, 114.9, 112.6, 109.5, 102.2, 83.2 HRMS (ESI−TOF) m/z Found 540.0790 [M − H]$^-$, calculated 540.0679, (+2.98 mmu).

DNAF2. 3,4-Dinitrobenzoic acid (23.5 mg, 0.11 mmol) was suspended in 6 mL of thionyl chloride and catalytic amount (a few drops, via a Pasteur pipet) of DMF was added. The mixture was refluxed for 3 h. Toluene (100 mL) was added to the reaction mixture, which was then evaporated in vacuo to dryness. The residue was dissolved in 5 mL of CH_2Cl_2 and cooled to −5 °C. A CH_2Cl_2 (2.5 mL) solution of 6-aminofluorescein dipivaloyl (53.5 mg, 0.10 mmol) and DIEA (50 μL, 0.30 mmol) was added dropwise, and the reaction mixture was stirred for 4 h at room temperature. The solvent was removed and the residue was redissolved in 10 mL of MeOH, then 10 mL of a solution of NaOMe (26 mg, 0.48 mmol) in MeOH was added dropwise with stirring overnight at room temperature. The reaction was quenched with 8 mL of aqueous 2 N HCl. The residue obtained by evaporation was purified by means of preparative reverse-phase HPLC to give the title compound, 7.4 mg (13% yield, orange solid). ^{1}H NMR (300 MHz, DMSO-d_6) δ: 11.03 (1H, s), 10.15 (2H, s), 8.68 (1H, d, J = 1.6 Hz), 8.41 (1H, dd, J = 8.4, 1. Six Hz), 8.37 (1H, d, J = 8.4 Hz), 8.06 (1H, dd, J = 8.4, 1.5 Hz), 8.02 (1H, d, J = 8.4 Hz), 7.64 (1H, d, J = 1.5 Hz), 6.68 (2H, d, J = 2.3 Hz), 6.64 (2H, d, J = 8.7 Hz), 6.57 (2H, dd, J = 8.7, 2.3 Hz). ^{13}C NMR (100 MHz, DMSO-d_6) δ: 168.2, 162.5, 159.5, 154.4, 151.7, 144.8, 143.4, 141.5, 139.1, 134.0, 129.1, 126.0, 125.8, 125.0, 121.7, 121.3, 113.9, 112.7, 109.4, 102.2, 82.3 HRMS (ESI−TOF) m/z Found 540.0656 [M − H]$^-$, calculated 540.0679, (−2.27 mmu).

NBDHEX. NBDHEX was synthesized from NBD-Cl and 6-mercapto-1-hexanol according to the literature[43] with minor modifications. ^{1}H NMR (300 MHz, $CDCl_3$) δ: 8.41 (1H, d, J = 7.9 Hz, a), 7.15 (1H, d, J = 8.1 Hz, b), 3.68 (2H, t, J = 6.3 Hz, h), 3.28 (2H, t, J = 7.3 Hz, c), 1.44−1.93 (8H, m, d-h) ^{13}C NMR (75 MHz, $CDCl_3$) δ 149.2, 142.5, 142.0, 132.5, 130.7, 120.2, 62.7, 32.4, 31.7, 28.6, 27.9, 25.3 HRMS (ESI^+) Calculated for $C_{12}H_{15}N_3NaO_4S$ (M + Na^+); 320.0681, found; 320.06557 (−2.52 mmu).

Synthesis of DNAT-Me. 2-Methyl-4-nitrobenzyl Alcohol (1). **1** was synthesized from 2-methyl-4-nitrobenzoic acid according to the literature.[44] ^{1}H NMR (300 MHz, DMSO-d_6) δ: 8.07 (1H, dd, J = 8.4, 2.3 Hz), 8.02 (1H, d, J = 2.3 Hz), 7.62 (1H, d, J = 8.4 Hz), 4.80 (2H, d, J = 5.4 Hz), 2.39 (3H, s,), 1.94 (1H, t, J = 5.4 Hz) ^{13}C NMR (100 MHz, $CDCl_3$) δ 147.1, 146.0, 136.9, 127.1, 121.2, 62.4, 18.6. LRMS (EI^+); 167.

2-Methyl-4-nitrobenzaldehyde (2). To a stirred CH_2Cl_2 solution (200 mL) containing pyridinium chlorochromate 3.4 g (15.9 mmol) and anhydrous magnesium sulfate 3.5 g, 1.41 g of **1** (8.4 mmol)

(43) Ricci, G.; De Maria, F.; Antonini, G.; Turella, P.; Bullo, A.; Stella, L.; Filomeni, G.; Federici, G.; Caccuri, A. M. *J. Biol. Chem.* **2005**, *280*, 26397–26405.

(44) Hay, M. P.; Sykes, B. M.; Denny, W. A.; O'Connor, C. J. *J. Chem. Soc., Perkin Trans. 1* **1999**, 2759–2770.

was added. The mixture was stirred for 6 h at ambient temperature. The organic solution was washed with water (100 mL × 3) and brine, dried over anhydrous sodium sulfate, and filtered. The filtrate was evaporated to dryness. The residue was purified on a silica gel column (Silicagel 60N, CH_2Cl_2/n-hexane = 4/1) to afford the title compound 1.15 g (83% yield, slight yellowish solid) ^{1}H NMR (300 MHz, $CDCl_3$) δ: 10.40 (1H, s), 8.19 (1H, dd, J = 8.3, 2.2 Hz), 8.15 (1H, d, J = 2.2 Hz), 7.99 (1H, d, J = 8.3 Hz), 2.80 (3H, s) ^{13}C NMR (75 MHz, $CDCl_3$) δ: 190.9, 150.2, 142.2, 137.9, 132.4, 126.6, 121.3, 19.5 LRMS (EI^+); 165.

4,4′-[(2-Methyl-4-nitrophenyl)methylene]bis(benzene-1,3-diol) (3). Resorcinol (1.4 g, 12.6 mmol) and 2-methoxy-4-nitrobenzaldehyde (**2**) (214.8 mg, 1.3 mmol) were dissolved in CH_2Cl_2/ether (1:1, 20 mL) and stirred at 4 °C. Methanesulfonic acid (2.0 mL) was added and the reaction mixture was stirred at ambient temperature for 15 min. The solution was evaporated and redissolved in ethyl acetate (100 mL). The organic solution was washed with water (100 mL × 3) and brine, dried over anhydrous Na_2SO_4, and filtered. The filtrate was evaporated to dryness. The residue was purified by a silica gel chromatography (Silicagel 60N, CH_2Cl_2/MeOH, 9:1) to give the title compound, 189 mg (40% yield, yellowish solid). ^{1}H NMR (300 MHz, CD_3OD) δ: 7.93 (1H, d, J = 2.3 Hz), 7.84 (1H, dd, J = 8.5, 2.3 Hz), 6.95 (1H, d, J = 8.5 Hz), 6.39 (2H, d, J = 8.3 Hz), 6.26 (2H, d, J = 2.4 Hz), 6.13 (2H, dd, J = 8.3, 2.4 Hz), 5.99 (1H, s), 2.23 (3H, s) ^{13}C NMR (100 MHz, CD_3OD) δ: 158.0, 157.1, 154.0, 147.2, 140.0, 131.4, 130.0, 125.4, 121.4, 121.2, 107.0, 103.5, 40.8, 19.6 HRMS (ESI−TOF) Calculated for $C_{20}H_{16}NO_6$ [M-H]$^-$; 366.0978, found; 366.0962 (−1.55 mmu).

6-Hydroxy-9-(2-methyl-4-aminophenyl)-3H-xanthen-3-one (2-Me-4-NH_2-TokyoGreen) (5). Compound **3** (106 mg, 0.29 mmol) and p-toluenesulfonic acid monohydrate (436 mg, 2.3 mmol) were suspended in 10 mL of dry toluene and heated to reflux (125 °C) for 14 h. After cooling to room temperature, the solution was neutralized with saturated sodium bicarbonate to pH = 7. The solution was acidified by dropwise addition of concentrated HCl to pH = 3−4. The precipitate was extracted into ethyl acetate (3 × 100 mL) and the solution was washed with brine (25 mL × 2). The combined organic extracts were dried over anhydrous sodium sulfate and the solvent was removed in vacuo. Silica gel column chromatography (Silicagel 60 (Wako), CH_2Cl_2/ MeOH, 9:1) afforded 6-hydroxy-9-(2-methyl-4-nitrophenyl)-3H-xanthen-3-one (**4**) (19.6 mg, crude). The identity of the product was confirmed by HPLC, and ESI-Tof-MS. A mixture of 92.8 mg of crude **4**, $Na_2S \cdot 9H_2O$ (598 mg, 2.5 mmol), and $NaSH \cdot nH_2O$ (440 mg) was heated in H_2O (50 mL) for 3 h under reflux. After cooling, the mixture was acidified with AcOH and the resulting dark red precipitate was collected, washed with cooled water and dried *in vacuo*, affording 28.4 mg of the title compound (3.0% yield in two steps, dark red solid). ^{1}H NMR (300 MHz, CD_3OD) δ: 7.66 (2H, d, J = 9.2 Hz), 7.26 (2H, d, J = 2.3 Hz), 7.18 (2H, d, J = 9.2, 2.3 Hz), 7.12 (1H, d, J = 8.3 Hz), 6.93−6.95 (1H, m), 6.90 (1H, dd, J = 8.3, 2.2 Hz), 1.99 (3H, s) ^{13}C NMR (100 MHz, CD_3OD) δ: 173.2, 166.9, 160.7, 150.2, 139.0, 134.7, 132.4, 122.5, 121.4, 118.6, 118.2, 114.3, 103.6, 20.2 HRMS (ESI^+) Calculated for $C_{20}H_{16}NO_3$ $[M + H]^+$; 318.1130, found; 318.1113 (−1.74 mmu).

DNAT-Me. A suspension of 3,4-dinitrobenzoic acid (42.1 mg, 0.20 mmol) in 5 mL of thionyl chloride was refluxed at 80 °C for 3 h. Then, 80 mL of toluene was added to the reaction mixture and evaporated *in vacuo* to dryness three times. The residue was dissolved to 4 mL of CH_2Cl_2, and cooled to 4 °C. A THF solution (2.5 mL) of 2-Me-4-NH_2-TokyoGreen (**5**) 17.3 mg (0.055 mmol) and DIEA (75 μL) was added dropwise, and the reaction mixture was stirred under an Ar atmosphere for 1.5 h at room temperature. The solvent was evaporated to dryness. The residue was dissolved in AcOEt and the resulting solution was washed with water and brine, dried over anhydrous Na_2SO_4, and filtered. The filtrate was evaporated to dryness. The residue was redissolved in 6 mL of methanol, and 10 mL of water (containing 1% triethylamine) was added. The reaction mixture was stirred at room temperature for 2 h, then acidified with 2 N HCl to pH 3−4. MeOH was evaporated, and the target compound was extracted with AcOEt (20 mL × 3). The organic layer was washed with brine, dried over anhydrous Na_2SO_4, and filtered. The mixture was lyophilized and purified by HPLC (buffer A; 100 mM triethylamine acetate (TEAA) buffer (pH 7.0), B; 80% CH_3CN/20% TEAA; eluted by running a gradient from 20−100% buffer B at an elution rate of 5 mL/min) to give a solution containing the title compound. This solution was acidified with AcOH and extracted with AcOEt (50 mL). The AcOEt solution was washed with brine, dried over anhydrous Na_2SO_4, and filtered. The filtrate was evaporated to give the title compound 2.4 mg (9% yield, red orange solid). ^{1}H NMR (400 MHz, DMSO-d_6) δ: 11.03 (1H, s), 8.86 (1H, dd, J = 1.5 Hz), 8.61 (1H, dd, J = 8.3, 1.5 Hz), 8.52 (1H, d, J = 8.3 Hz), 7.97 (1H, d, J = 2.0 Hz), 7.93 (2H, dd, J = 8.3, 2.0 Hz), 7.38 (1H, d, J = 8.3 Hz), 6.97 (2H, d, J = 9.3 Hz), 6.80−6.53 (4H, m), 2.11 (3H, s) ^{13}C NMR (100 MHz, DMSO-d_6) δ 171.6, 163.1, 158.6, 152.9, 151.2, 149.2, 148.9, 145.9, 143.4, 139.6, 139.3, 137.7, 135.6, 134.5, 131.3, 127.5, 109.6, 29.0 HRMS (ESI^-) Calculated for $C_{27}H_{16}N_3O_8$ $[M - H]^-$; 510.0938, found; 510.0940 (+0.29 mmu).

Expression and Purification of GSTs. cDNA clones of human GSTA1 and GSTM1 were purchased from ATCC. pET-21a(+) and pET-21b(+) plasmid DNAs were purchased from Novagen. Cloning of pET-GST was conducted according to general cloning procedures. Overexpression of human GSTs was achieved by transforming *Escherichia coli* BL21 (DE3) cells with pET-21b(+)-hGSTA1, pET-21a(+)-T7-hGSTM1, and pET-21b(+)-hGSTP1, respectively. A single colony was inoculate into 5 mL of 2 × YT supplemented with ampicillin (100 mg/mL) and grown overnight at 37 °C with shaking. This overnight seed culture was then used to inoculate 1 L of fresh growth medium and grown at 37 °C until induction with isopropyl thio-β-D-galactoside (IPTG) (1.0 mM final concentration). After agitation for 3 h at 37 °C, the cells were collected by centrifugation. The cells were suspended in working solution (50 mM phosphate, 300 mM NaCl) and sonicated. (10 pulses of 20s, on ice). Cell debris was removed by centrifugation at 10 000 rpm for 60 min at 4 °C, after which the cell lysate supernatant was transferred to swollen glutathione agarose, which was stirred slowly at 4 °C. The mixture was washed with buffer A (3 mM EDTA, 20 mM potassium phosphate (pH 7.0), and 3 mM mercaptoethanol) and centrifuged (1000 rpm, 3 min), and these processes were repeated ten times. GSTs were eluted with GSH solution (10 mM GSH, 50 mM Tris (hydroxymethyl) aminomethane, 0.4 M NaCl). The eluate was dialysed against buffer A overnight, then buffer B (3 mM EDTA, 20 mM potassium phosphate (pH 7.0), 3 mM 2-mercaptoethanol, 20% glycerol) for 6 h. Purified GSTs were checked by SDS-PAGE (acrylamide 12.5%).

GST Specific Activity Measurement. GST assays with CDNB as a substrate were performed on a C-550 UV/vis spectrophotometer equipped with a stirrer controller and water bath (EYELA NCB-120) maintained at 25 °C. The standard assay mixture contained 1.0 mM GSH, 1.0 mM CDNB (2% EtOH as a cosolvent), and 0.1 mM EDTA in 3 mL of 100 mM potassium phosphate buffer, pH 6.5. The activity was determined spectrophotometrically at 340 nm ($\epsilon = 9.6\ mM^{-1}\ cm^{-1}$) within 20 s after substrate addition. Reported enzymatic specific activities are the averages of three independent determinations at three different concentrations of enzyme in the range where concentration−initial rate proportionality was maintained. Assays with DNAFs as a substrate were performed at 37 °C. The standard assay mixture contained 1.0 mM GSH, 0.5 μM **DNAF1** or **2** (0.1% DMSO as a cosolvent), and phosphate-buffered saline (PBS, pH 7.4). The activity was determined spectrophotometrically at 514 nm with excitation at 490 nm. The rate of product formation was estimated by use of the equation, Initial rate = $P \times (F_t - F_0)/\{t \times (F_{Max} - F_0)\}$, where F_t and F_0 represent the fluorescence at times t and 0 min, P is the amount of product of a known concentration in solution, and F_{Max} is the fluorescence due to P of product. Reported enzymatic specific activities are the

averages of three independent determinations at three different concentrations of enzyme in the range where concentration-initial rate proportionality was maintained. The determined values of specific activity are shown at Table 2.

Kinetic Parameter Measurement. NNBA. GST assays were performed at 37 °C. NNBA in the concentration range of 3−100 mM (each with 1% DMSO as a cosolvent), 1.0 mM GSH, and 0.241 μg/mL hGSTP1 were used. The activity was determined spectrophotometrically at 381 nm (product absorption, $\epsilon = 3$ mM^{-1} cm^{-1}) based on the reported method.[45] Michaelis−Menten (MM) plots were approximated with KaleidaGraph (Synergy Software, Reading, PA). From the resulting MM plots, k_{cat} and K_M were obtained. Second-order rate constants were calculated from the results in the absence of GST.

mBBr. GST assay was performed at 37 °C. mBBr in the concentration ranging 2.5−25 μM (each with 1% EtOH as a cosolvent), 1.0 mM GSH, and an appropriate concentration of GSTs were used in PBS (pH 7.4). The activity was determined spectrophotometrically at 470 nm (excited at 400 nm) within 100 s after addition of the substrate.

DNAFs. GST assays were performed at 37 °C. Assay conditions were the same as described for GST specific activity measurement except that initial rate values were derived from the averages of three different DNAF concentrations in the range of 0.5−1.5 μM. Because quenching of fluorescence owing to the inner filter effect occurs at high concentrations of fluorogenic substrate, we calculated approximate k_{cat}/K_M values directly. The apparent k_{cat}/K_M was derived using the MM relationship at low DNAF concentrations (0.5−1.5 μM): $v/([E]*[S]) = k_{cat}/K_M$, when $K_M > [S]$. Both substrates displayed linear rate vs substrate concentration behavior in this concentration region.

Measurement of Released Nitrite. Nitrite released from NNBA was measured with a NO_2/NO_3 Assay Kit-C II (Colorimetric) Griess Reagent Kit (Dojindo, Japan) according to the manufacturer's instructions. Briefly, the kinetic measurement assays were done with NNBA in the concentration range of 6.25−100 μM. In the plateau phase of the reaction, the reaction mixtures were transferred to a 96-well plate. Using known concentrations of nitrite as a standard, the concentration of released nitrite was determined with a SH-8000 (Laboratory) Micro plate reader (Corona Electric Co., Ltd., Tsukuba, Japan).

Cells Lines and Culture Conditions. Human cholangiocarcinoma cell line HuCCT1 and a cell line derived from normal lung, OUS11, were purchased from the Health Science Research Resources Bank (Osaka, Japan). Human leukemia cell line HL-60 and human fibrosarcoma cell line HT1080 were purchased from RIKEN Bioresource Center cell bank (Tsukuba, Japan). HuCCT1 and HL-60 were cultured in RPMI 1640 medium (Sigma) containing 10% fetal bovine serum (Invitrogen) and penicillin/streptomycin, and OUS 11 was cultured in minimum essential medium (Invitrogen) containing 10% fetal calf serum (Invitrogen) and penicillin/streptomycin. Human cervical adenocarcinoma cell line HeLa was cultured in Dulbecco's modified Eagle's medium (Invitrogen) containing 10% fetal bovine serum and penicillin/streptomycin.

All cell lines were maintained at 37 °C in an atmosphere of air containing 5% CO_2.

Microscopic Imaging. For fluorescence imaging of GST activity in living cells, DNAT-Me was used at a final concentration of 2 μM in Hanks' buffered salt solution (HBSS), pH 7.4. Imaging experiments with HuCCT1 cells were conducted at two days after seeding. Cells were washed with PBS twice and incubated in HBSS, containing the vehicle or 5 μM CCCP or 50 μM *N*-ethylmaleimide (NEM) (0.1% DMSO as a cosolvent) for 15 min at 37 °C. Then, the medium was replaced with new HBSS solution containing 2 μM DNAT-Me (0.3% DMSO as a cosolvent) in the control experiment. In the case of CCCP or NEM treatment, the medium was replaced with new HBSS solution containing 2 μM DNAT-Me and 5 μM CCCP or 50 μM NEM (0.3% DMSO as a cosolvent) and incubated for a further 15 min at 37 °C. (In the confocal overlay experiment with SYTO, HBSS containing 2 μM DNAT-Me, 5 μM CCCP, and 1 μM SYTO 60-red (0.4% DMSO as a cosolvent) was used.) Fluorescence images were captured using an Olympus IX 71 with a cooled CCD camera (Coolsnap HQ, Olympus), a xenon lamp (AH2RX-T, Olympus) with a BP-470−490 excitation filter, and a BA 510−550 emission filter. In the confocal microscopic experiment, fluorescence images were captured using an Olympus Fluoview system withg an IX81 inverted microscope, an argon ion laser and HeNe laser, and a PlanApo 40×/1.00 objective lens (Olympus). The excitation wavelength was 488 nm, and the emission was detected via an FITC filter for DNAT-Me. For SYTO 60-red, the excitation wavelength was 633 nm and the emission was detected via a Cy-5 filter.

Acknowledgment. We thank our colleagues Suguru Kemmoku, Tasuku Ueno, Takuji Shoda, and Akira Yastushige for helpful discussions, Eri Ikeda and Yosuke Kaku for their kind assistance with molecular cloning technique, and Nae Saito for UPLC−MS analysis. This study was supported in part by research grants (Grant Nos. 19021010 and 19205021) to Y.U., and a grant for the Advanced and Innovational Research Program in Life Sciences to T.N. from the Ministry of Education, Culture, Sports, Science and Technology of the Japanese Government, and grants from Hoansha Foundation to T.N.

Supporting Information Available: Specific activities toward CDNB and DNAFs; molecular structures of evaluated substrates for GST; ^{1}H NMR chart of the NNBA before and after glutathionylation; spectra of DNAFs and DNAT-Me before and after glutathionylation; fluorescence timecourse of reactions between DNAF1 and various thiol compounds and lysine derivatives; inhibitor evaluation; HPLC chromatograms of DNAT-Me loaded cell lysate; and additional microscopic image.This material is available free of charge via the Internet at http://pubs.acs.org.

JA802423N

(45) Morgenstern, R.; Lundqvist, G.; Hancock, V.; Depierre, W. *J. Biol. Chem.* **1988**, *263*, 6671–6675.